INTERFACE

rsif.royalsocietypublishing.org

Research

Cite this article: Hawkes EW, Eason EV, Christensen DL, Cutkosky MR. 2015 Human climbing with efficiently scaled gecko-inspired dry adhesives. *J. R. Soc. Interface* **12**: 20140675.
http://dx.doi.org/10.1098/rsif.2014.0675

Received: 26 June 2014
Accepted: 27 October 2014

Subject Areas:
biomimetics

Keywords:
adhesion, scaling, gecko, climbing, bioinspiration

Author for correspondence:
Elliot W. Hawkes
e-mail: ewhawkes@stanford.edu

Electronic supplementary material is available at http://dx.doi.org/10.1098/rsif.2014.0675 or via http://rsif.royalsocietypublishing.org.

THE ROYAL SOCIETY PUBLISHING

Human climbing with efficiently scaled gecko-inspired dry adhesives

Elliot W. Hawkes[1], Eric V. Eason[2], David L. Christensen[1] and Mark R. Cutkosky[1]

[1]Department of Mechanical Engineering, and [2]Department of Applied Physics, Stanford University, Stanford, CA 94305, USA

Since the discovery of the mechanism of adhesion in geckos, many synthetic dry adhesives have been developed with desirable gecko-like properties such as reusability, directionality, self-cleaning ability, rough surface adhesion and high adhesive stress. However, fully exploiting these adhesives in practical applications at different length scales requires efficient scaling (i.e. with little loss in adhesion as area grows). Just as natural gecko adhesives have been used as a benchmark for synthetic materials, so can gecko adhesion systems provide a baseline for scaling efficiency. In the tokay gecko (*Gekko gecko*), a scaling power law has been reported relating the maximum shear stress σ_{max} to the area A: $\sigma_{max} \propto A^{-1/4}$. We present a mechanical concept which improves upon the gecko's non-uniform load-sharing and results in a nearly even load distribution over multiple patches of gecko-inspired adhesive. We created a synthetic adhesion system incorporating this concept which shows efficient scaling across four orders of magnitude of area, yielding an improved scaling power law: $\sigma_{max} \propto A^{-1/50}$. Furthermore, we found that the synthetic adhesion system does not fail catastrophically when a simulated failure is induced on a portion of the adhesive. In a practical demonstration, the synthetic adhesion system enabled a 70 kg human to climb vertical glass with 140 cm^2 of adhesive per hand.

1. Introduction

Over a decade ago, scientists first reported the mechanism of adhesion in geckos. These animals exploit a complex hierarchical adhesion system, using nanoscale fibres which produce adhesion through van der Waals forces and can be attached and detached by controlling the loading angle [1]. Since then, researchers have created bioinspired adhesives using silicones, urethanes, plastics, carbon nanotubes and other materials; these materials boast impressive gecko-like properties such as reusability, self-cleaning ability, controllability, rough surface adhesion and the capability to produce large adhesive stresses [2,3]. While the thrust of the research has been on developing and testing such properties in small-scale laboratory tests, in order to fully exploit these adhesives at different length scales, it is necessary to achieve efficient scaling, i.e. an increase in adhesive area without a significant decrease in adhesive capabilities.

The length scale on which we focus in this work is the human scale, motivated by the challenge of human climbing with a gecko-inspired dry adhesive. The adhesive chosen for this task consists of polydimethylsiloxane (PDMS) slanted microwedges (roughly 100 μm tall), which adhere well to glass and can be repositioned many times without degradation [4,5] (figure 1, inset). While other dry adhesive materials produce larger adhesive stresses, PDMS microwedges are especially suitable for climbing because they exhibit *controllable adhesion* that can be effectively switched on or off in a fraction of a second by applying a shear stress. Therefore, a climber can attach PDMS microwedges simply by transferring weight to the adhesive, and can detach by removing the weight, requiring nearly-zero added effort. However, this work, on efficient scaling, is not specific to PDMS microwedges and may be applicable to a wide range of other adhesive materials.

There have been notable efforts to scale adhesives beyond small laboratory tests, but there has been little work dealing specifically with scaling efficiency. Researchers have created small robots that climb well with dry adhesives [7–11],

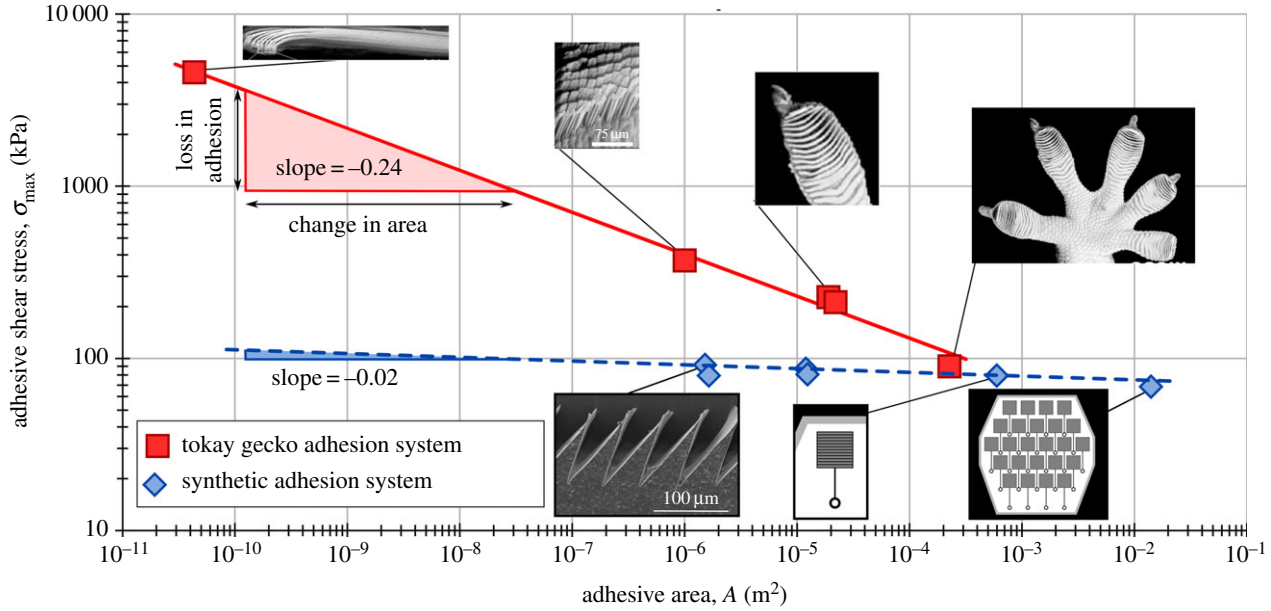

Figure 1. The red squares ($n = 5$) indicate the maximum adhesive shear stress σ_{max} that can be achieved on a flat, smooth surface by tokay gecko adhesion systems as the adhesive area A increases [6]. From left, these data correspond to a single seta, a setal array, a toe and two feet. The red line shows the least-squares power law fit to the data (log $\sigma_{max} = -0.24 \log A + 1.1$). Similarly, for the PDMS microwedge synthetic adhesion system, the blue diamonds ($n = 6$) represent the maximum adhesive stress produced by a 1.5 mm^2 patch, a 12 mm^2 patch, a 6.5 cm^2 tile and a 24-tile system. The least-squares power law is plotted as a blue dashed line (log $\sigma_{max} = -0.02 \log A + 1.8$).

yet these systems cannot support as large a load as predicted by their total area of adhesive. For instance, Stickybot had an area of adhesive that should have supported 5 kg based on small-scale tests, but could only support 500 g owing to inefficient scaling [11]. In other work, adhesive anchors capable of holding impressive loads have been created [12,13], but the scaling efficiency of these adhesion systems has not been reported. Additionally, a demonstration of human climbing with gecko-inspired adhesives has been recently revealed by the Defense Advanced Research Projects Agency (DARPA) Z-Man programme [14], but details of the adhesive material, climbing device and total area of adhesive remain undisclosed.

Without scaling efficiency numbers in the literature, it is useful to set a scaling efficiency benchmark by turning towards the adhesion systems of geckos, as designers of dry adhesives have done previously to judge the relative merits of their synthetic materials. In the tokay gecko (*Gekko gecko*), the adhesion decreases as the length scale increases from the seta-scale to the toe- and foot-scale [6]. This adhesion system has been found to approximately follow a scaling power law, $\sigma_{max} \propto A^{-1/4}$, where σ_{max} is the maximum shear stress supported by the adhesive and A is the adhesive area (figure 1, red squares).

If the benchmark power law of the tokay gecko were applied to the PDMS microwedge adhesive, an impractically large area of more than 1200 cm^2 of adhesive per hand would be required to support a 70 kg human climber with no safety factor (a modern tennis racket is approx. 675 cm^2). This is partly because the area of adhesive required for climbing increases disproportionately as the scale increases (even with perfectly efficient scaling) owing to the climber's surface area and mass following a square-cube law.

Therefore, to allow a human to climb with a practical area of controllable dry adhesive, it is necessary to attain significantly more efficient scaling than that of the gecko's adhesion system. To achieve this goal, we developed a synthetic adhesion system which ensures that the load distribution across a large adhesive area is nearly uniform, using a concept referred to as *degressive load-sharing*. In degressive load-sharing, elastic elements which have decreasing stiffness with increasing displacement support independent patches of adhesive and help equalize the load on all patches. The synthetic adhesion system was found to sustain adhesive stress with little decrease across four orders of magnitude of area, approximately following the power law $\sigma_{max} \propto A^{-1/50}$ (figure 1, blue diamonds). Furthermore, the system was found to resist catastrophic failure by preventing stress concentrations when a simulated failure was induced on a portion of the adhesive (see §2.3), and the system also requires little effort to attach or detach (see §2.5). Thus, with efficient scaling, robustness to failure and controllable adhesion, the synthetic adhesion system enables a human to ascend a vertical glass surface with a hand-sized[1] area of adhesive (figure 2).

2. Results

2.1. Gecko stress distribution data

To aid the comparison of the synthetic adhesion system and the adhesion system of the tokay gecko, we developed a sensor to take *in vivo* measurements of the stress distributions on gecko toes (see appendix A.1 and Eason *et al*. [16]). The adhesion sensor data for a tokay gecko toe on a flat surface (figure 3*a*) show that very little of the useful adhesive area was working at maximum capacity. Only a fraction of the adhesive area contacted the surface, and the load was not evenly distributed even in the areas that did make contact. Similar results were also observed for a different species (crested gecko, *Correlophus ciliatus*), as shown in figure 3*b*. These results suggest that load-sharing in gecko adhesion systems may not be ideal, which motivates the development of a synthetic system with improved load-sharing.

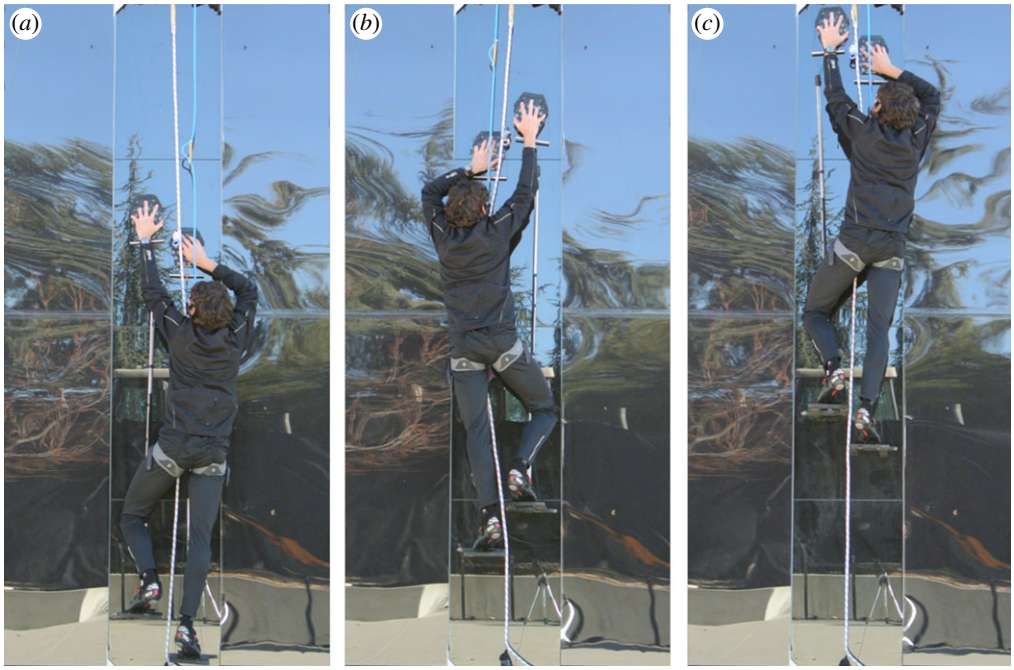

Figure 2. Three frames from a video (electronic supplementary material, movie S1) showing a 70 kg climber ascending a 3.7 m vertical glass surface using a synthetic adhesion system with degressive load-sharing and gecko-inspired adhesives. The time between (*a*) and (*c*) is about 90 s and includes six steps.

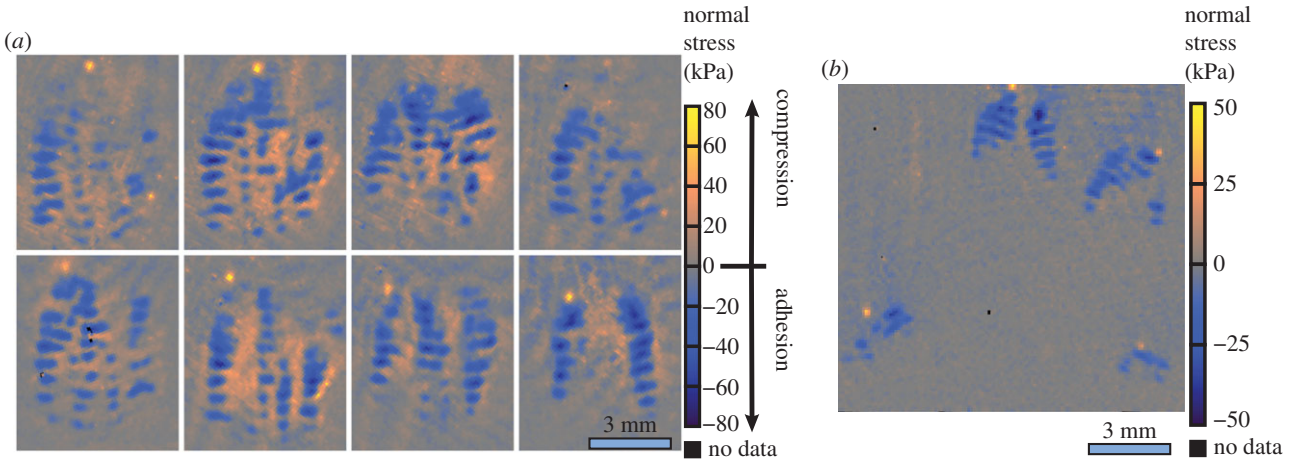

Figure 3. Measured load distributions of gecko toes *in vivo*. (*a*) Tactile sensor data of the third toe of the right hind foot of a tokay gecko on a flat surface, showing the normal stress distribution just before the onset of slip (appendix A.1). Only a fraction of the adhesive area produced large adhesive stresses, indicating that load-sharing in the gecko's toe is not ideal. (*b*) Data for a crested gecko showing similar results. (Online version in colour.)

2.2. Degressive load-sharing concept

The human climbing synthetic adhesion system presented here retains several gecko-inspired design features, such as controllable adhesives [1], the separation of the adhesive into discrete elements [17] (with the tiles in the synthetic adhesion system corresponding to lamellae in geckos) and a load-bearing structure that is compliant normal to the surface yet comparatively stiff in the loading direction [18]. Each tile of adhesive is loaded using a tendon-like string. In order to ensure that the stress distribution is uniform over each tile, the tendons are attached so that they do not apply moments to the tiles, and the tiles are made rigid to prevent deflection [9]. Because rigid tiles cannot conform to large curvature, an array of smaller tiles performs significantly better than a single large tile on surfaces that are insufficiently flat (figure 9). Therefore, the adhesive is divided into 24 independent tiles to make the synthetic adhesive system functional on practical surfaces. This necessitates the use of a load-sharing mechanism to distribute the total load among the tiles.

In general, load-sharing is accomplished by a suspension that applies forces to patches of adhesive. In the tokay gecko, this suspension is composed primarily of the stratum compactum of the skin of each lamella, which comprises taut elastin and coiled collagen fibres [17]. During extension, the stiffness of the skin increases as the collagen uncoils and bears load. This is equivalent to a *progressive* elastic element (i.e. an element with tangent stiffness that increases with displacement), as shown in figure 4*a* [19]. However, a progressive element is not ideal for load-sharing. If some random variation in displacement exists among the patches of adhesive, the progressive stiffness curve will cause the subsequent variation in shear loads to become magnified as the displacements increase. Using a simple model (see appendix A.2), we predict that a synthetic adhesive system with suitable progressive elements

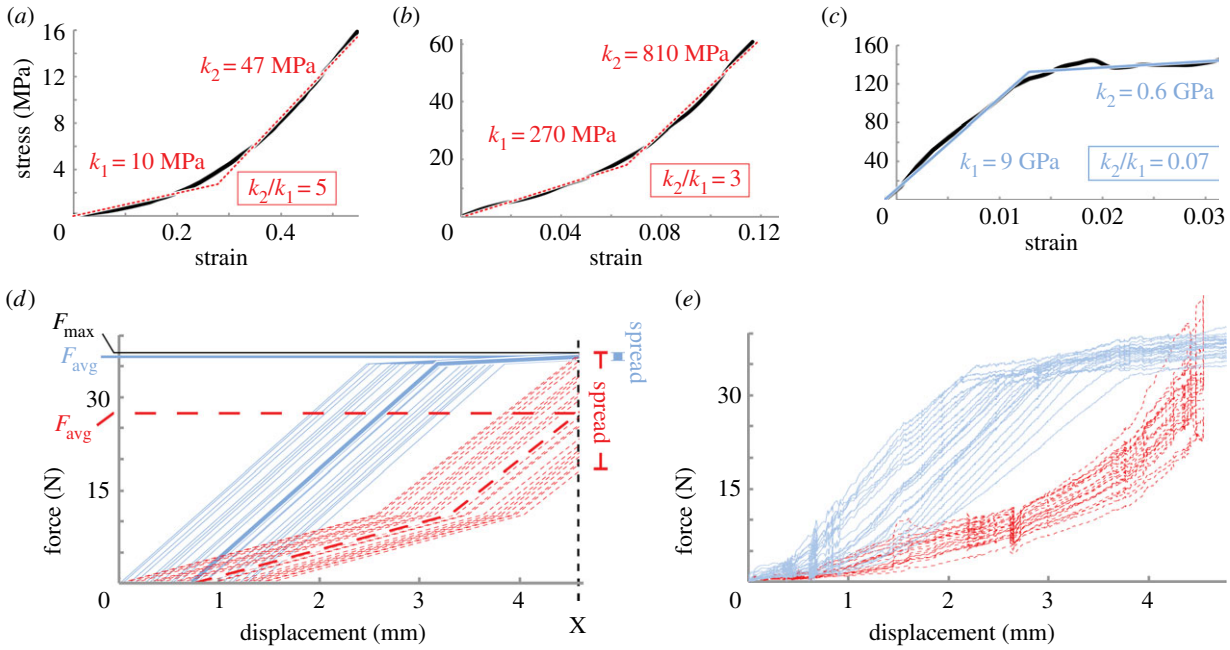

Figure 4. Effects of progressive and degressive elastic elements in load-sharing. (*a*) Stress–strain curve of the skin of the tokay gecko [19], with a piecewise linear fit shown in dashed red. The ratio of k_2 to k_1 is 5, corresponding to a *progressive* elastic element. (*b*) Stress–strain curve of a strand of extruded nylon, with a k_2 to k_1 ratio of 3, used as a *progressive* element for testing in the synthetic device. (*c*) Stress–strain curve of a superelastic nitinol wire, with ratio of k_2 to k_1 of 0.07, corresponding to a *degressive* elastic element. (*d*) A simple model based on identical nonlinear springs loaded in parallel with different initial displacements predicts the behaviour of synthetic progressive springs (dashed red) and synthetic degressive springs (solid blue) when used to load 24 adhesive patches. The initial displacement offsets were measured from the synthetic adhesion system (appendix A.2). At the maximum displacement $x = 4.6$ mm, the spread in forces is predicted to be much larger for the progressive springs than for the degressive nitinol springs. The average forces F_{avg} are 74% and 97% of the maximum force F_{max} for the two cases. (*e*) Force and displacement data from the synthetic adhesion system with progressive nylon springs (dotted red) and degressive nitinol springs (solid blue) (electronic supplementary material, Methods, force and displacement sensor). At the displacement $x = 4.6$ mm, the average force F_{avg} for the progressive springs was 70% of the maximum force F_{max}, but 94% for the degressive nitinol springs.

would result in an average adhesive force on all of the tiles that is only 74% of the maximum force on any of the tiles (figure 4*d*, dashed red lines).

Instead of using a biomimetic load-sharing system with progressive elastic elements, the synthetic adhesion system uses *degressive* elastic elements. Unlike most materials, degressive elements become more compliant with extension while remaining elastic. Here, we use elements made of superelastic nitinol which exhibit a roughly 15-fold decrease in stiffness over the range of extension, as shown in figure 4*c*. Using degressive elements as suspensions for patches of adhesive results in a decrease in the variation in adhesive loads as the displacements increase. In the low-stiffness regime, the elements produce a nearly-constant force over a large range of displacements, so variations in displacement are decoupled from variations in force. Unlike very soft, linear springs, degressive elements require only a small amount of total displacement to achieve an even load distribution. Additionally, as long as at least one element is still in its high-stiffness regime, the system exhibits high stiffness. Thus, the synthetic adhesion system 'feels' stiff, although many of the parallel elements are in a low-stiffness regime. If all the elements are in the low-stiffness regime, the overall stiffness of the system is much lower, but there is no instability, because the stiffness is still positive.

With degressive load-sharing, our model now predicts an average adhesive force that is 97% of the maximum (figure 4*d*, solid blue lines). Force and displacement measurements from the 24-tile synthetic adhesion system with progressive and degressive load-sharing elements (figure 4*e*) show that the average adhesive forces at maximum extension were 70% and 94% of the maximum force on any of the tiles, in good agreement with the model. The uniformity of the force distribution can be quantified by the ratio of the standard deviation to the mean, or coefficient of variation (CV), which was roughly constant for the progressive elements, but significantly decreased near maximum extension for the degressive elements (figure 5). The degressive elements are tuned, so that they enter the low-stiffness (nearly-constant force) regime at a force just below the maximum force the PDMS microwedge adhesive on each tile can support as predicted by small-scale tests. Thus, when the synthetic adhesion system reaches maximum extension, the stress distribution over the adhesive area is both uniform and maximized, ensuring efficient scaling.

2.3. System stability with degressive load-sharing

While scaling efficiency is an important metric, for practical adhesion systems, the system stability and robustness to failure are equally important. If a small section of the adhesive detaches from the surface, does the entire system catastrophically fail?

A similar question is considered in fracture mechanics, when a solid fails at a stress far below that predicted by ultimate strength after a crack is introduced. Accordingly, researchers have used Griffith crack theory [20] to model the phenomenon that occurs when an elastic block adhered to a surface peels after a small section becomes unbonded, with the 'crack' at the interface between the elastic block and the adherend surface [21]. This peeling phenomenon can cause an adhesion system to fail at a stress far below the theoretical maximum.

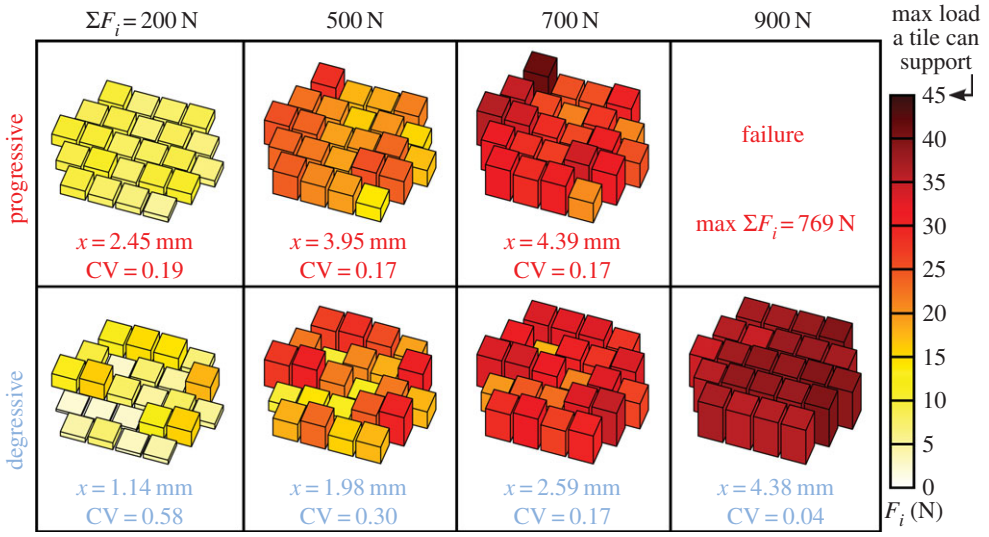

Figure 5. Visualizations of the synthetic adhesion system force–displacement data from figure 4*e* at selected values of the total force, using either progressive or degressive load-sharing elements. The CV, equal to the ratio of the standard deviation to the mean ($n = 24$), remained constant at a moderate value (0.17–0.19) for the progressive elements as the load increased, but decreased significantly for the degressive elements (ending at 0.04). Near maximum load, the force distribution was non-uniform in the progressive case, with a few tiles carrying disproportionately high percentages of the load; on the other hand, the distribution became highly uniform in the degressive case near maximum load, with all of the tiles supporting nearly equal forces. As a result, the degressive springs enabled the system to support a higher total force before exceeding the failure threshold of the tiles. (Online version in colour.)

One method to inhibit crack propagation in peeling adhesive films is to attach the adhesive to a backing layer that is stiff in the loading direction [13]. Another method is to array the adhesive material into elastically coupled sections [22,23], which tends to halt, divert and reinitiate the crack.

While both these methods are effective at decreasing the propensity of a crack to propagate, peeling still occurs in general, because the stress is concentrated along the crack front. On the other hand, a different situation occurs for a system of adhesive tiles loaded through independent degressive elements. If an adhesive tile fails, the combined load on the other tiles must increase to compensate for the decrease in area. However, this stress increase is not necessarily concentrated in the area surrounding the failure. The load is increased only on degressive elements that have not yet reached the nearly-constant-force regime. The loads on the other tiles do not increase, even if they are next to the tile that failed, because they are elastically decoupled from each other owing to the low stiffness and independent nature of the degressive elements. Interestingly, the loads on the tiles remaining on the surface become more evenly distributed instead of more concentrated. This behaviour continues as long as the load is not large enough to put all degressive elements into their nearly-constant-force regimes.

The synthetic adhesion system exhibited this stable behaviour in tests. An array of seven tiles was placed on a grid of force sensors and loaded to about 75% of the maximum load for the array. Next, one of the tiles was slowly unloaded, simulating a slip failure. This type of failure could be caused by a contaminated or damaged tile or surface. As the tile was unloaded, the force it had been carrying was transferred to the two tiles that had been supporting less than 30 N of load, whereas the force on the highly loaded tiles did not change significantly (figure 6). Because the highly loaded tiles did not experience a substantial increase in force, they did not become overloaded and the failure did not propagate.

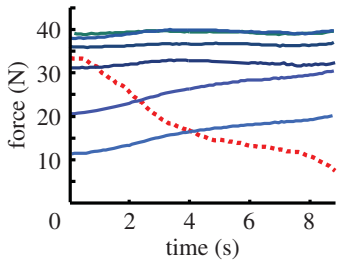

Figure 6. Robustness to failure of degressive load-sharing mechanism. Forces produced by seven adhesive tiles are plotted with respect to time. When one tile was unloaded, as during a slipping failure (dotted line), the forces on the tiles with the largest loads (greater than 30 N) remained constant, whereas the forces on the tiles with lower loads took up the majority of the force no longer supported by the unloaded tile. This is in contrast to systems without degressive load-sharing, where stresses increase locally near failed areas, leading to crack-like failure propagation. Forces were measured using the apparatus described in electronic supplementary material, Methods, force and displacement sensor. (Online version in colour.)

As a final note on stability, the superelastic nitinol degressive elements employed in the synthetic adhesion system have a hysteretic behaviour. This means that when a tile fails, less energy is released from its degressive element than was put in, resulting in a relatively smaller disturbance to the system than would occur with non-hysteretic elements.

2.4. Further modifications to the gecko's adhesion system

In addition to degressive load-sharing, the synthetic adhesion system has other design elements which are modified from the equivalent parts of the gecko adhesion system to improve performance. First, the structure of the load-bearing tendons was modified. In the tokay gecko, the lateral digital tendons split into branches, each of which inserts into an individual lamella and loads an independent patch of adhesive

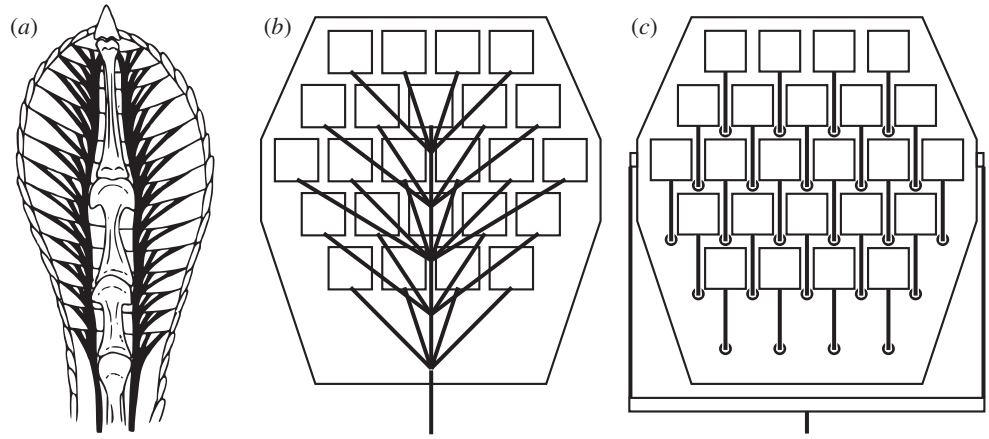

Figure 7. Comparison of the branched network of tendons in a gecko toe (*a*) (reproduced with permission from Russell [24]), a biomimetic branched design (*b*) and the parallel network of tendons used in the synthetic adhesion system (*c*). Owing to the components of the tendon forces that are perpendicular to the external load, the biomimetic design would support only 82% of the external load that the parallel tendon design holds, solely considering tendon geometry differences.

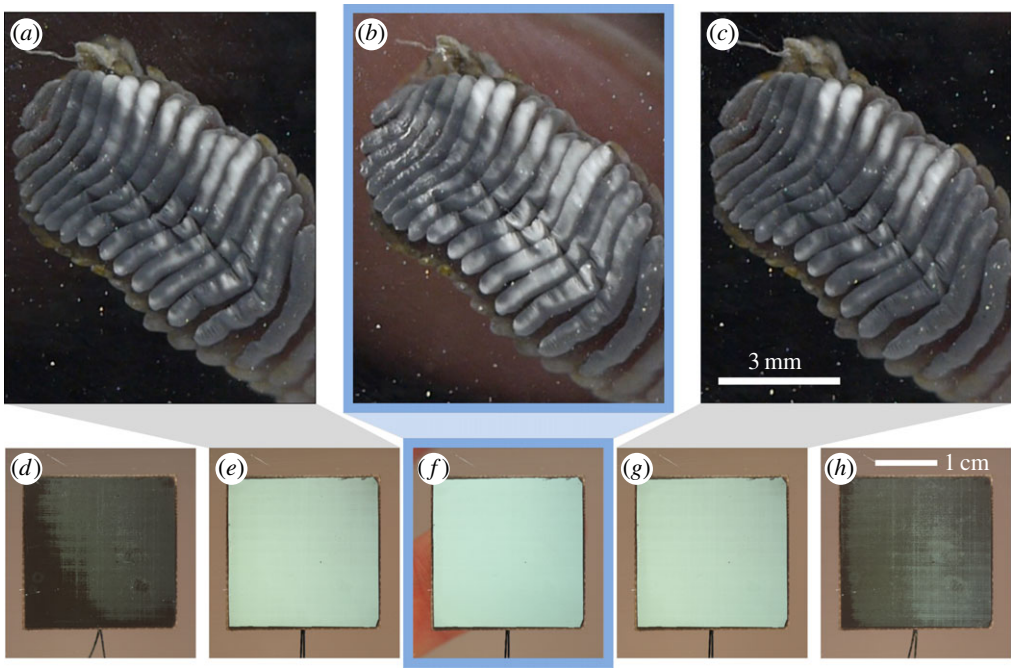

Figure 8. Contact area of a gecko toe and an adhesive tile under load, measured using frustrated total internal reflection (FTIR). (*a–c*) Three frames from a video of a tokay gecko toe on an FTIR sensor (appendix A.1 and the electronic supplementary material, movie S2). The gecko first placed its toe and loaded it (*a*). Next, pressure was applied manually to the dorsal surface of the toe, greatly increasing the contact area (*b*). Finally, the pressure was removed, and the contact area decreased (*c*). The real areas of contact (normalized to the compressed state) were 49.7%, 100%, and 35.3% for (*a*), (*b*) and (*c*), respectively. (*d–h*) When one of the adhesive tiles from the synthetic adhesion system was set on the FTIR sensor (*d*), then loaded through a tendon (*e*), it came fully into contact. Pressure on the back of the tile (*f*) did not increase the contact area, nor did the contact area decrease when the pressure was removed (*g*). However, when the load in the tendon was removed, the contact area greatly decreased and the adhesive released from the surface (*h*). (Online version in colour.)

(figure 7*a*) [24]. Such a branched design allows the transfer of load solely through tension, without requiring compressive or bending elements, which could prevent a structure from conforming to non-flat surfaces. However, any branch that is at an angle with respect to the external load vector has a component of tension that does not contribute to the external load. Because we know, *a priori*, that our intended climbing surface is relatively flat, we are able to include compressive and bending elements to make all of the tendons parallel (figure 7*c*). Considering only tendon geometry, this parallel design can support 22% more load than a biomimetic branched design (figure 7*b*).

Second, we increased the flatness of the adhesive patches to improve adhesion on flat surfaces. If the shape of the adhesive surface is not identical to the shape of the adherend surface, non-uniform adhesive stresses are required to maintain contact across the entire area. In certain areas, these stresses may be above the adhesive limit causing the adhesive to detach. We observed spontaneous detachment for portions of a tokay gecko toe on a flat surface (figure 8*a–c*), suggesting that the stresses required to flatten the adhesive surface are greater than the gecko's adhesive limit in certain areas of the toe. This is not ideal for adhesion on flat surfaces. As explanation for this behaviour, we note that tokay geckos have been shown to perform well on slightly undulating substrates [25], and we conjecture that the tokay adhesion system is adapted for use on non-flat surfaces which may be more common in the tokay gecko's natural habitat.

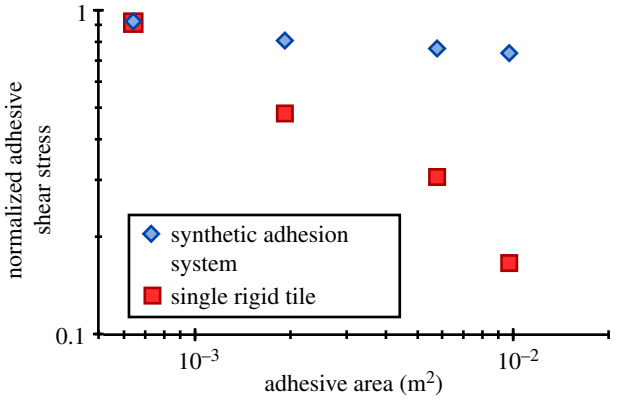

Figure 9. Scaling behaviour of the synthetic adhesion system on a slightly curved ($\rho \approx 200$ m) acrylic surface (blue diamonds). Area was adjusted by varying the number of adhesive tiles in the system. Adhesive performance data of single rigid adhesive tiles of different sizes on this surface are included for comparison (red squares). Performance values are normalized relative to the force per unit area of the adhesive on flat acrylic. (Online version in colour.)

In contrast, the synthetic adhesion system uses adhesive patches that are optimized for flat surfaces. The adhesive patches are mounted on rigid flat tiles, which deviate from flatness by no more than the working distance of the PDMS microwedge adhesive features (35 µm) over the length of the tiles (2.5 cm); additionally, the tiles are sufficiently rigid to maintain this flatness tolerance when loads are applied [9]. Using rigid flat tiles avoids internal elastic stresses in the adhesive backing and allows nearly-complete contact area without stress concentrations when loaded on a flat surface (figure 8*d–h*).

2.5. Adhesion system capabilities

With these design features, the synthetic adhesion system was found to produce a nearly-uniform load distribution (figure 5) and a much more efficient scaling behaviour than that of the gecko with little decrease in adhesive ability across four orders of magnitude of area ($\sigma_{max} \propto A^{-1/50}$ (figure 1). The synthetic adhesion system also exhibits good scaling on surfaces with some curvature ($\rho \approx 200$ m; figure 9), in contrast to a simple single-tile mechanism. On this curved surface, the synthetic system with area of 100 cm^2 performs at just under 80% of the performance of a 6.5 cm^2 tile on a flat surface, whereas a 100 cm^2 single tile achieves only approximately 15%. Using this system, a human of mass 70 kg successfully ascended a 3.7 m vertical glass wall with 140 cm^2 of gecko-inspired dry adhesives in each hand (figure 2). We tested hundreds of individual steps on glass with the 70 kg climber and 140 cm^2 of adhesive without failure. In addition, we tested the maximum load for the system five times, finding an average of 95.6 kg (938 N) and a standard deviation of 2.7 kg (26 N). Finally, we found that the compressive force required to preload the device before loading is small (less than 1 N) and that the force required to release the device after unloading is also small (less than 2 N). Thus, the system retains the property of controllability from the adhesive material.

3. Discussion

We have shown that a synthetic adhesion system using degressive load-sharing elements distributes loads uniformly and robustly and allows efficient scaling of adhesives. In addition, we demonstrated the feasibility of applying the synthetic adhesion system to human climbing. However, these conclusions are made with some qualifications.

First, the *in vivo* gecko measurements are incomplete owing to the use of only two individual test subjects (one of each species). These results should be regarded as suggestive rather than as conclusive, as it is possible that the measured stress distributions may have been influenced by the geckos' behaviour, stage in their moulting cycle, human handling or individual anatomical variations.

Second, while the synthetic adhesion system may be able to outperform a gecko on relatively flat, smooth and clean vertical glass, on other surfaces, it has poor performance compared with the gecko. However, it may be possible to partially overcome these design limitations. To adhere to surfaces with more curvature, the tile size could be decreased at the expense of greater system complexity; and for rougher surfaces, the adhesion system could be outfitted with one of the gecko-inspired adhesive materials that have been developed for use on these surfaces. On contaminated surfaces, even geckos have trouble producing adhesion (van der Waals forces require intimate contact between the surface and the adhesive); however, gecko adhesive has been observed to self-clean when it becomes contaminated [26]. The PDMS microwedge adhesive can be cleaned between steps by touching a material of higher surface energy (e.g. sticky tape), and it may be possible to achieve self-cleaning using an even lower-surface-energy, harder material, and by adopting finer terminal features [27].

Third, degressive load-sharing involves a trade-off between uniformity of the load distribution and robustness to failure. Maximum uniformity is achieved at maximum extension of the degressive elements, at which point a failure could potentially be catastrophic. The failure-tolerant load redistribution behaviour described in §2.3 is only possible at less than maximum extension, when at least one of the adhesive loads is below maximum. While degressive load-sharing does not always ensure exactly equal loads, it does ensure that all loads are limited to a safe level as long as the entire system is not overloaded. The load limits are determined by the low-stiffness regime of the degressive elements. For degressive load-sharing to function correctly, these limits must be preset according to the maximum adhesion attainable on the intended combination of adhesive and adherend surface.

Fourth, it is unknown whether the performance of the synthetic adhesion system can be extended to yet larger scales. It is of interest to determine whether a system can be created that continues the adhesive capability power law to the 0.1 or 1 m^2 size scale; such an adhesion system could support unprecedented amounts of force. For example, if the power law in figure 1 holds, a system 10 times larger (0.14 m^2) could hold approximately 9.5 times the load (915 kg).

Further improvements to the synthetic adhesion system are possible. The climbing speed was limited by the posture of the climber, not by the adhesion system (which can attach and detach in less than a second), so further work optimizing the climbing device for human biomechanics is warranted. In addition, the synthetic adhesion system may be suitable for other practical applications besides climbing. The current system can support loads on a fixed vertical wall, but further testing will be necessary to determine the feasibility of using the adhesion system in grasping or manipulation applications. Recent work has also shown that PDMS microwedges function in the environment of outer space [28], so it would be of interest to test this adhesion system in such an environment.

4. Conclusion

Considerable research has been dedicated to creating gecko-inspired adhesives with desirable properties, but little work has been directed towards efficient scaling: scaling adhesives to large areas for practical applications with almost equal performance at all scales. We have developed a synthetic adhesion system that allows efficient scaling over four orders of magnitude of area. The synthetic adhesion system creates a nearly-uniform load distribution across the whole adhesive area, improving upon the adhesive-bearing structures of a gecko's toe and enabling a human to climb vertical glass using an area of adhesive no larger than the area of a human hand. These results show that gecko-inspired adhesives can be scaled from laboratory-scale tests to human-scale applications with little decrease in performance.

Acknowledgements. The PDMS microwedge adhesive technology used in this work was developed in collaboration with the DARPA Z-Man programme. We thank Jon Renslo and Marc Windheim for building sensors. We thank Tom Libby (CiBER, University of California, Berkeley) for handling the geckos for the experiments. We thank Benjamin Tee and Alex Chortos for supplying micro-pyramids for the tactile sensor. We thank Kellar Autumn for photos of the gecko adhesion system.

Funding statement. E.W.H. was supported by a National Science Foundation Graduate Research Fellowship. E.V.E. was supported by a Hertz Fellowship, Stanford Graduate Fellowship, and National Science Foundation Graduate Research Fellowship. D.L.C. was supported by SRI and DARPA HR0011-12-C-0040.

Endnotes

[1]An average adult male hand has a palmar surface area of about 140–170 cm^2 [15].

[2]$x = 4.6$ mm is equal to the intertile spacing: a total displacement larger than this would result in tiles colliding in the case of one tile detaching from the surface while all the rest remain in contact. Such a collision could result in the contacted tile failing, and the failure would propagate.

Appendix A. Methods

A.1. *In vivo* measurements of gecko adhesion

The trend of decreasing adhesive capability with increasing area observed in the tokay gecko (figure 1) has not been fully explained. It has been suggested that this is partially caused by a reduction in contact area or unequal load-sharing between or within lamellae [6,29], but no measurements supporting this have been presented. Therefore, we investigated this question by measuring the stress distribution on gecko toes *in vivo*. The distance between lamellae is only 500–600 µm for the tokay gecko, so we built a custom optical tactile sensor with 100 µm spatial resolution.

The sensor was orientated vertically and an adult tokay gecko of body mass 101.2 g voluntarily attached to the sensor with its right hind foot. The gecko was oriented head downwards and was pulled off the sensor manually. While the human interaction in the test adds uncertainty, it was necessary, because the gecko's body weight was not large enough to test the limits of its adhesive; furthermore, a similar method has been previously reported [1]. This test was repeated with varying pull angles to obtain different stress distributions on the foot. Selected stress distributions for the third toe are shown in figure 3*a* at points in time immediately preceding large-scale slip. For further details about this measurement, see the electronic supplementary material, Methods and reference [16].

This test was repeated with an adult crested gecko, which was instead oriented head upwards. The gecko placed its right front foot on the sensor, and was pulled off the sensor manually. A selected stress distribution from this test is shown in figure 3*b*.

In addition, the area of contact of the tokay gecko was measured using frustrated total internal reflection (FTIR) within a rectangular acrylic waveguide. This technique has been used to measure the area of contact of gecko-inspired adhesives [30]. After the gecko placed its foot on the waveguide, we manually applied and removed a compressive force to the toes, which caused the contact area to increase and decrease as shown in figure 8*a–c*. A video recorded during this test is presented in the electronic supplementary material, movie S2.

All animal testing was done at the Center for Interdisciplinary Bio-inspiration in Education and Research (CiBER) in full compliance with the regulations of UC Berkeley. UC Berkeley is a USDA-registered research facility, maintains a Public Health Service (PHS) Animal Welfare Assurance, and has been fully accredited by the Association for Assessment and Accreditation of Laboratory Animal Care, International (AAALAC) continuously since 1994. UCB maintains full compliance with the US Public Health Service Policy on Humane Care and Use of Laboratory Animals (PHS Policy), the National Research Council's Guide for the Care and Use of Laboratory Animals and the US Department of Agriculture's Animal Welfare Act Regulations regarding the care and use of animals in a research setting.

A.2. Load-sharing model

The model used to create figure 4*d* involves an array of identical nonlinear springs loaded in parallel, where the initial displacements of the springs are distributed over some range. Each spring follows the same force–displacement curve,

$$F_i = f(x - Q_i), \tag{A 1}$$

where F_i is the force on the ith patch of adhesive, f is the force–displacement curve of the springs used, x is the displacement of the entire system, and Q_i is the relative displacement between the ith patch and the patch with the tautest tendon. The maximum force F_{max} occurs for the patch with the tautest tendon ($Q_{min} = 0$), and is given by equation (A 2),

$$F_{max} = f(x). \tag{A 2}$$

Assuming the function $f(X)$ is linear over the range of possible values taken by $X = x - Q_i$, then

$$F_{avg} = F_{max} - k(x)Q_{avg}, \tag{A 3}$$

where $k(x) = df/dx$ is the tangent stiffness of the springs at the displacement x (i.e. k_2 for the piecewise linear fits in figure 4*a–c*).

In order to compare the progressive and degressive springs, we used this model to calculate the maximum and average forces that would result from using the two types of springs in the 24-tile synthetic adhesion system. The force–displacement curves $f(x)$ of a degressive nitinol wire and a progressive strand of nylon fishing line were directly measured. The dimensions of these elastic elements were chosen, so that they produced the same force at $x = 4.6$ mm, which is the maximum

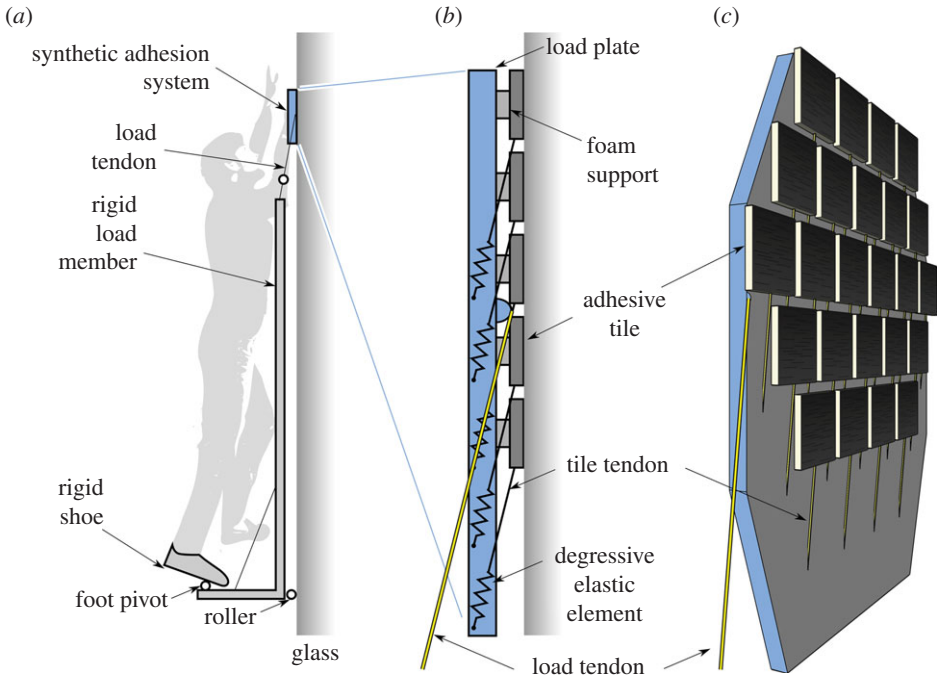

Figure 10. Design of the climbing device and the synthetic adhesion system. (*a*) Climbing device: the load is transferred from the synthetic adhesion system through the load tendon into the rigid load member, which lies along the surface out of the way of the climber and supports the climber at the foot pivot. A rubberized roller prevents sideslip, and the foot pivot allows the ankle joint to be used. The foot pivot is located away from the wall, which allows the climber to move his or her centre of mass closer to the wall than the foot pivot, negating any tendency to fall backwards. (*b*,*c*) Synthetic adhesion system: the load is transferred from the adhesive tiles, through the tile tendons, into the degressive elastic elements, through the load plate and into the load tendon. The soft foam supports hold the adhesive tiles in place while in the swing phase, but are of negligible stiffness during the stance phase. The total area of the adhesive is 140 cm^2 on each hand, divided into 24 independent tiles of dimensions 2.5 × 2.5 cm. (Online version in colour.)

displacement of the synthetic adhesion system.[2] The initial displacements Q_i were determined from the degressive-spring experimental data in figure 4*e* by measuring the different values of x that resulted in each tile producing 10 N.

Using the progressive force–displacement curve of the nylon strand, equations (A 2) and (A 3) predict $F_{max} = 37$ N and $F_{avg} = 27\ \text{N} = 0.74\ F_{max}$ (figure 4*d*, dashed red lines). With the degressive nitinol springs and with the same x and Q_{avg}, the model predicts $F_{max} = 37$ N and $F_{avg} = 36\ \text{N} = 0.97\ F_{max}$ (figure 4*d*, solid blue lines).

A.3. System design

The designs of the synthetic adhesion system and human climbing device are illustrated in figure 10. The device is designed so that the climber's weight is supported by the leg muscles instead of the weaker upper body. The climber's hands are used to place the adhesive on the wall, but the load is then transferred through a system of tendons and load members to the climber's shoes. Each hand controls an independent 24-tile synthetic adhesion system which supports the corresponding foot during each stride.

The synthetic adhesion system contains 24 independent adhesive tiles in a staggered grid. Each tile is a 2.5 × 2.5 cm square and is attached to an independent degressive elastic element (figure 10*b*,*c*). The climbing device and synthetic adhesion system are designed so that the angle of the overall load on the synthetic adhesion system and the angles of the individual loads on the tiles remain between 0° and 7° from vertical. This improves the maximum load that the PDMS microwedge adhesive can support. Details of the design and construction of the system are provided in the electronic supplementary material, Methods.

References

1. Autumn K *et al*. 2002 Evidence for van der Waals adhesion in gecko setae. *Proc. Natl Acad. Sci. USA* **99**, 12 252–12 256. (doi:10.1073/pnas.192252799)
2. Sameoto D, Menon C. 2010 Recent advances in the fabrication and adhesion testing of biomimetic dry adhesives. *Smart Mater. Struct.* **19**, 103001. (doi:10.1088/0964-1726/19/10/103001)
3. Hu S, Xia Z, Dai L. 2013 Advanced gecko-foot-mimetic dry adhesives based on carbon nanotubes. *Nanoscale* **5**, 475–486. (doi:10.1039/c2nr33027j)
4. Day P, Eason EV, Esparza N, Christensen D, Cutkosky MR. 2013 Microwedge machining for the manufacture of directional dry adhesives. *J. Micro Nano-Manuf.* **1**, 011001. (doi:10.1115/1.4023161)
5. Parness A, Soto D, Esparza N, Gravish N, Wilkinson M, Autumn K, Cutkosky M. 2009 A microfabricated wedge-shaped adhesive array displaying gecko-like dynamic adhesion, directionality and long lifetime. *J. R. Soc. Interface* **6**, 1223–1232. (doi:10.1098/rsif.2009.0048)
6. Autumn K. 2006 Properties, principles and parameters of the gecko adhesive system. In *Biological adhesives* (eds AM Smith, JA Callow), pp. 225–256. Berlin, Germany: Springer.
7. Daltorio KA, Wei TE, Horchler AD, Southard L, Wile GD, Quinn RD, Gorb SN, Ritzmann RE. 2009 Mini-Whegs™ climbs steep surfaces using insect-inspired attachment mechanisms. *Int. J. Robot. Res.* **28**, 285–302. (doi:10.1177/0278364908095334)
8. Murphy MP, Kute C, Mengüç Y, Sitti M. 2011 Waalbot II: adhesion recovery and improved

performance of a climbing robot using fibrillar adhesives. *Int. J. Robot. Res.* **30**, 118–133. (doi:10.1177/0278364910382862)

9. Hawkes EW, Eason EV, Asbeck AT, Cutkosky MR. 2013 The gecko's toe: scaling directional adhesives for climbing applications. *IEEE/ASME Trans. Mech.* **18**, 518–526. (doi:10.1109/TMECH.2012.2209672)
10. Krahn J, Liu Y, Sadeghi A, Menon C. 2011 A tailless timing belt climbing platform utilizing dry adhesives with mushroom caps. *Smart Mater. Struct.* **20**, 115021. (doi:10.1088/0964-1726/20/11/115021)
11. Kim S, Spenko M, Trujillo S, Heyneman B, Santos D, Cutkosky MR. 2008 Smooth vertical surface climbing with directional adhesion. *IEEE Trans. Robot* **24**, 65–74. (doi:10.1109/TRO.2007.909786)
12. Heepe L, Kovalev AE, Varenberg M, Tuma J, Gorb SN. 2012 First mushroom-shaped adhesive microstructure: a review. *Theor. Appl. Mech. Lett.* **2**, 014008. (doi:10.1063/2.1201408)
13. Bartlett MD, Croll AB, King DR, Paret BM, Irschick DJ, Crosby AJ. 2012 Looking beyond fibrillar features to scale gecko-like adhesion. *Adv. Mater.* **24**, 1078–1083. (doi:10.1002/adma.201104191)
14. Defense Advanced Research Projects Agency. 2014 DARPA Z-Man program demonstrates human climbing like geckos. See http://www.darpa.mil/NewsEvents/Releases/2014/06/05.aspx (accessed 10 June 2014).
15. Hsu YW, Yu CY. 2010 Hand surface area estimation formula using 3D anthropometry. *J. Occup. Environ. Hyg.* **7**, 633–639. (doi:10.1080/15459624.2010.514259)
16. Eason EV, Hawkes EW, Windheim M, Christensen DL, Libby T, Cutkosky MR. In press. Stress distribution and contact area measurements of a gecko toe using a high-resolution tactile sensor. *Bioinspir. Biomim.*
17. Russell AP. 1986 The morphological basis of weight-bearing in the scansors of the tokay gecko (Reptilia: Sauria). *Can. J. Zool.* **64**, 948–955. (doi:10.1139/z86-144)
18. Russell AP. 1981 Descriptive and functional anatomy of the digital vascular system of the tokay, Gekko gecko. *J. Morphol.* **169**, 293–323. (doi:10.1002/jmor.1051690305)
19. Bauer AM, Russell AP, Shadwick RE. 1989 Mechanical properties and morphological correlates of fragile skin in gekkonid lizards. *J. Exp. Biol.* **145**, 79–102.
20. Griffith AA. 1921 The phenomena of rupture and flow in solids. *Phil. Trans. R. Soc. Lond. A* **221**, 163–198. (doi:10.1098/rsta.1921.0006)
21. Gao H, Yao H. 2004 Shape insensitive optimal adhesion of nanoscale fibrillar structures. *Proc. Natl Acad. Sci. USA* **101**, 7851–7856. (doi:10.1073/pnas.0400757101)
22. Ge L, Sethi S, Ci L, Ajayan PM, Dhinojwala A. 2007 Carbon nanotube-based synthetic gecko tapes. *Proc. Natl Acad. Sci. USA* **104**, 10 792–10 795. (doi:10.1073/pnas.0703505104)
23. Glassmaker NJ, Jagota A, Hui CY, Noderer WL, Chaudhury MK. 2007 Biologically inspired crack trapping for enhanced adhesion. *Proc. Natl Acad. Sci. USA* **104** 10 786–10 791. (doi:10.1073/pnas.0703762104)
24. Russell AP. 1975 A contribution to the functional analysis of the foot of the tokay, Gekko gecko (Reptilia: Gekkonidae). *J. Zool.* **176**, 437–476. (doi:10.1111/j.1469-7998.1975.tb03215.x)
25. Gillies AG, Henry A, Lin H, Ren A, Shiuan K, Fearing RS, Full RJ. 2014 Gecko toe and lamellar shear adhesion on macroscopic, engineered rough surfaces. *J. Exp. Biol.* **217**, 283–289. (doi:10.1242/jeb.092015)
26. Hansen WR, Autumn K. 2005 Evidence for self-cleaning in gecko setae. *Proc. Natl Acad. Sci. USA* **102**, 385–389. (doi:10.1073/pnas.0408304102)
27. Lee J, Fearing RS. 2008 Contact self-cleaning of synthetic gecko adhesive from polymer microfibers. *Langmuir* **24**, 10 587–10 591. (doi:10.1021/la8021485)
28. Parness A *et al*. 2013 Controllable on-off adhesion for Earth orbit grappling applications. In *2013 IEEE Aerospace Conf*. New York, NY: IEEE.
29. Bullock JM, Federle W. 2011 Beetle adhesive hairs differ in stiffness and stickiness: *in vivo* adhesion measurements on individual setae. *Naturwissenschaften* **98**, 381–387. (doi:10.1007/s00114-011-0781-4)
30. Lee J, Fearing RS, Komvopoulos K. 2008 Directional adhesion of gecko-inspired angled microfiber arrays. *Appl. Phys. Lett.* **93**, 191910. (doi:10.1063/1.3006334)